

Effect of Laser Irradiation on structure, Morphology and gas Sensor Properties of Chemical Spray Pyrolysis Deposited Nanostructured In_2O_3 Films

Ali A. Yousif*

Zainab S. Mahdi*

Abstract

In this study, Indium oxide nanocrystalline In_2O_3 films have been successfully deposited on glass substrates by Chemical Spray Pyrolysis (CSP) technique at substrate temperature of (300°C) It was irradiated by pulses N_2 laser at different power average (0.85, 1.70, 2.125 and 2.55mW). The structural and sensitivity properties of these films have been investigated using XRD, AFM and the sensitivity to NO_2 gas in air ambient has been measured in gas sensing system. The XRD results showed that all films are polycrystalline in nature with cubic structure and preferred orientation along (321) plane. The crystallite size was calculated using scherrer formula. The crystallite size of the samples was maximum (17.5nm) before irradiation, and it was minimum (8.04nm) at power average (2.55mw), prepared at the same films. AFM results showed homogenous and smooth Indium oxide thin films. The average grain size, average roughness and root mean square (RMS) roughness for nanocrystalline In_2O_3 films were estimated from AFM. The sensitivity of nanocrystalline In_2O_3 films to NO_2 gas in air ambient has been measured in gas sensing system. All samples were tested at different power average, and bias voltage (6 volt). The optimal operating temperature is found to be 300°C for In_2O_3 films for the maximum sensitivity is (64.12%) at power average (1.70mw), with fast response time (5.85s) and recovery time of (9.0s) at power average (0.85mw).

Key words: Laser Irradiations, Nanocrystalline In_2O_3 , Structure and sensitivity Properties, CSP.

1. Introduction

Indium oxide is a wide band gap semiconductor commonly employed as transparent electrode material in electrochromic windows, flat panel displays, organic light-emitting diodes and solar cells [1–6]. Metal oxide semiconductor films are widely applied in gas sensors. The properties of such sensors including sensitivity, selectivity and response time depend critically on the film microstructure [7]. The structure in turn is largely determined by the synthesis. Such films are usually synthesized by a variety of techniques including Spray Pyrolysis Technique (SPT) [8], sol-gel technique [9], and chemical vapor deposition [10]. A number of studies have shown that one promising approach to improve conduct metric metal oxide sensors is to utilize semiconducting nanostructured composite materials consisting of metal oxides with different electronic structure and chemical properties [11]. It has been established that using a mixture of metal oxides, the resulting composite sensor material can achieve selectivity and sensitivity for gas detection in air ambience that far exceed those achievable with the individual constituent metal

oxides of the composite [12]. In the present work, Indium oxide (In_2O_3) thin films have been prepared using chemical spray pyrolysis method, the objective of this work is to investigate the tuning of structural properties and gas sensing of samples after irradiation by pulses NO_2 laser at different power average.

2. Experiment

Chemical spray pyrolysis method was employed in the present work, where in this method, thin films were prepared by spraying the solution on a hot glass substrate at a certain temperature, and the film could be then obtained by the chemical reaction on the hot substrate. However, in some application these thin films could have good properties, for example. It might be used in solar and sensor applications.

The spraying solution which contains the materials necessary for fabrication of the InCl_3 film can be prepared by mixing Indium chloride InCl_3 and thiourea $\text{CS}(\text{NH}_2)_2$ as starting materials. The molar concentration of the solution should be equal to 0.1 mole/liter. In order to prepare the solution of 0.1 molar concentrations from these two materials, 0.5529 grams weight of InCl_3 and 0.190 grams weight of $\text{CS}(\text{NH}_2)_2$ are needed from each of them, melted in 50 ml of distilled water, according to the following equation:

$$\text{Weight of the material (gm)} = \text{Volume (ml)} \times \text{Molecular concentration (mol/l)} \times \text{Molecular weight (gm/mol)} \quad \dots\dots\dots (1)$$

$$\text{The weight of } \text{InCl}_3 = (50/1000) \times 0.1 \times 0.5529 = 0.00276 \text{ gm.}$$

$$\text{The weight of } \text{CS}(\text{NH}_2)_2 = (50/1000) \times 0.1 \times 0.190 = 0.00095 \text{ gm.}$$

Finally, the two weights materials melted in (50 ml) of distilled water to get the wanted solution (The spray solution). The solution then sprayed and deposited on a cleaned glass (300°C) substrate to get the finally In_2O_3 thin films. It is necessary to leave the glass substrate on the electrical heater for one hour at least after finishing the operation of spraying to complete its oxidation and crystalline growth process. The nanocrystalline were irradiated with one shot of laser beam of 10ns pulse and different power average (0.85, 1.70, 2.125 and 2.55mW) from N_2 laser system at 337 nm wavelength.

A. Laser Irradiation nitrogen (N_2) Technique

Nitrogen laser are important because they can provide high –power short- duration pulses of ultraviolet radiation ($\lambda=337.1 \text{ nm}$). These laser are widely used in pumping dye laser, spectroscopy and fluorescence studies, fast speed photography, etc.

In the present work, Indium oxide (In_2O_3) thin films have been prepared using chemical spray pyrolysis method, and irradiated pulses laser N_2 with different power average (0.85, 1.70, 2.125 and 2.55mW) for irradiation time (5min) and Pulse width (2.5ns) and Peak power (100kw) made in Germany that was used for the first time in the Ministry of Science and Technology in Iraq.

B. X-Ray Diffraction

In order to explain the structural properties, the nature and the crystal growth of the deposited films at different depositing conditions, x-ray diffraction measurement has been done according to the JCPD date for In_2O_3 nanocryst, were examined by X-ray diffractions using a(XR-DIFRACTOMETER/6000) type Shimadzu X-ray diffract meter system. This system recorded the intensity as a function of Bragg's angle. The measurement conditions are as follows: Target: CuK_α , Wavelength = 1.5406Å, Voltage = 40 Kv, Current = 30 mA, Scanning angle: (20- 80°) and Scanning Speed = 5 (degree/min).

While, the average crystallite size of the films can be estimated by the Scherrer formula using the full width at half-maximum (FWHM) value of the XRD diffraction peaks.

C. Atomic Force Microscopy

The surface morphology, particle size distribution and Root Mean Square (RMS) of roughness of In_2O_3 films prepared under various condition were analyzed using Atomic Force Microscope (AFM), (Nanosurf Flex AFM). The Atomic Force Microscopy is a member of the family of scanning probe microscopes which has grown steadily since the invention of the scanning tunneling microscope by Binning and Quate. The AFM measures the forces acting between a fine tip and a sample. The tip is attached to the free end of a cantilever and is brought very close to the surface. Attractive or repulsive forces resulting from interactions between the tip and the surface will cause a positive or negative bending of the cantilever.

D. Gas Sensor Measurements

In order to determine the sensitivity parameter mainly the response time and recovery time of In_2O_3 films before and after laser irradiation with different power average, suitable setup is prepared for this purpose, which it consists of : cylindrical stainless steel test chamber of diameter 21cm and of height 22cm with. A multi pin feed through at the base of the chamber allows the electrical connections to be established to the heater, K-type thermocouple, and sensor electrodes.

The heater consists of a hot plate and a K-type thermocouple inside the chamber in order to control the operating temperature of the sensor. A PC-interfaced digital Multimate of type UNI-T UT81B, and Laptop PC, is used to register the variation of the sensor current when exposed to air- NO_2 gas mixing ratio. The mixing is 3% NO_2 gas and 97% air, the mixing gas is feeding through a

tube over the sensor inside the test chamber to give the real sensitivity. The thin films surface exposed to 6ppm vapor concentrations of Nitrogen dioxide gas.

3. Results and Discussion

A. Structural Properties

1. XRD Spectra

The XRD spectrum of both unirradiated and laser irradiated of In₂O₃ films, in figure (1) suggesting cubic phase (JCPDS card, No. 44-1087). It is seen that the peaks are more broadened and shifted toward the decrease in diffraction angle when the film is exposure to laser irradiations.

The XRD pattern shown in figure (1) suggests that the In₂O₃ films polycrystalline in nanocrystalline In₂O₃ films (Cubic phase). Decrease in size of the particles is also observed as calculated from Scherrer relation before and after laser irradiation. Usually, the crystallite size calculated through Scherrer formula is smaller. This is attributed to the widening of the XRD peak due to internal stress and defects [13]. The intensities of first six characteristic peaks (310), (321), (411), (431), (521) and (037) almost reduced to half with increase in the broadening (FWHM) in case of laser irradiated samples. But when you increase the power average to 2.125 and 2.55mW, note the low intensity dramatically with the disappearance of some of the peaks and tend to the amorphous.

The expansion and deformation of the sample are attributed to the thermal effect caused by the localized surface plasmon resonances [14]. Particle size of the crystallites size of the crystals in the sample before and after laser irradiation is calculated from XRD patterns using following well-known Scherrer's formula calculated using the relation: [15]

$$D = \frac{0.9\lambda}{\Delta_{(2\theta)} \cos \theta} \dots\dots\dots(2)$$

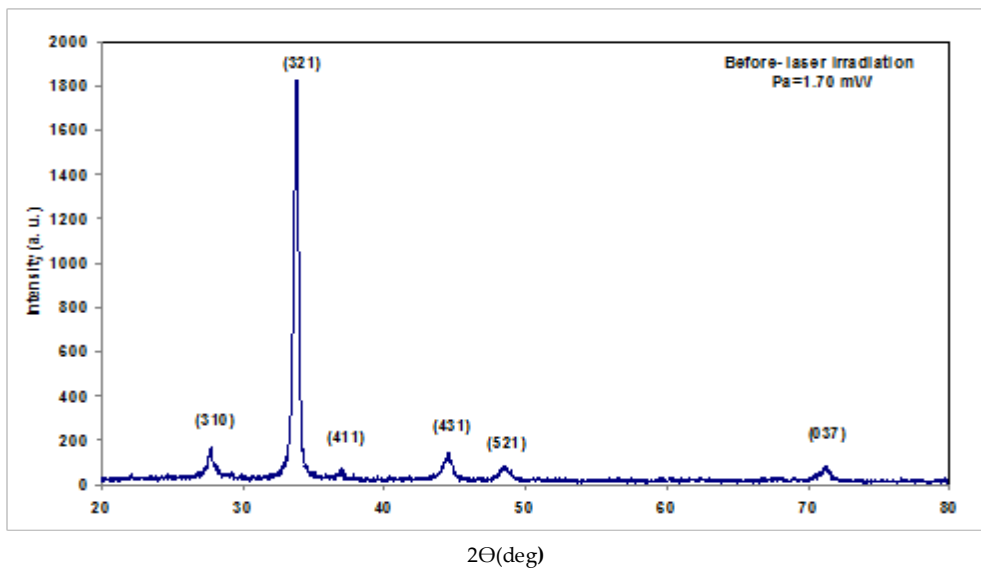
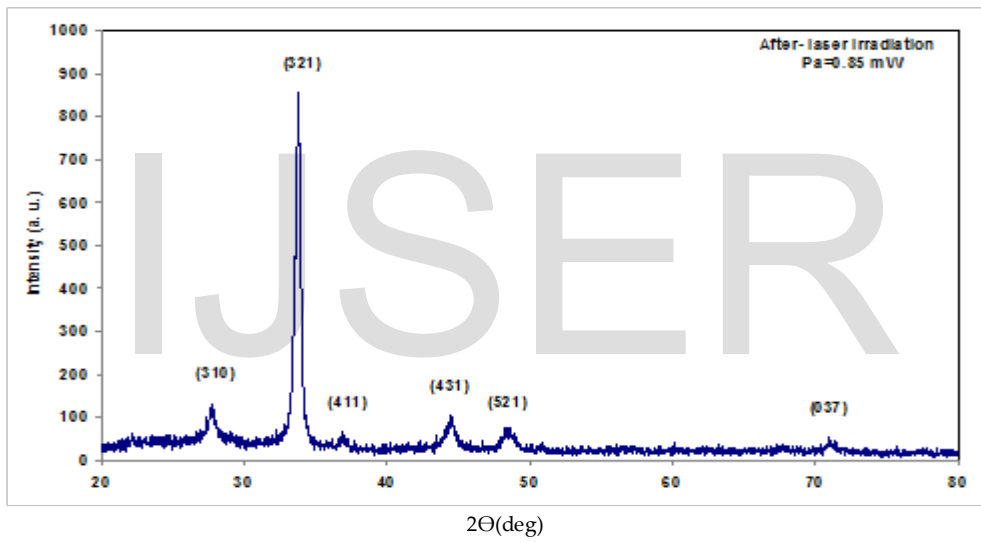
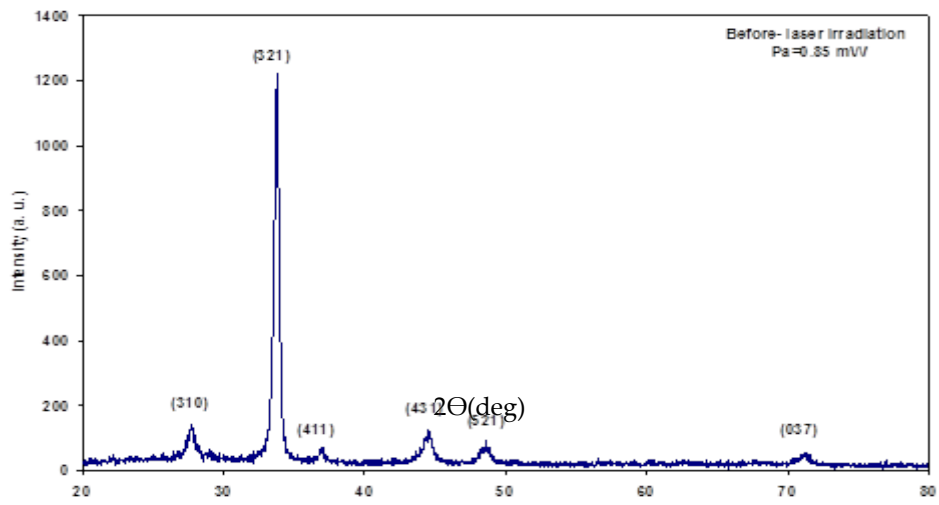
Where:

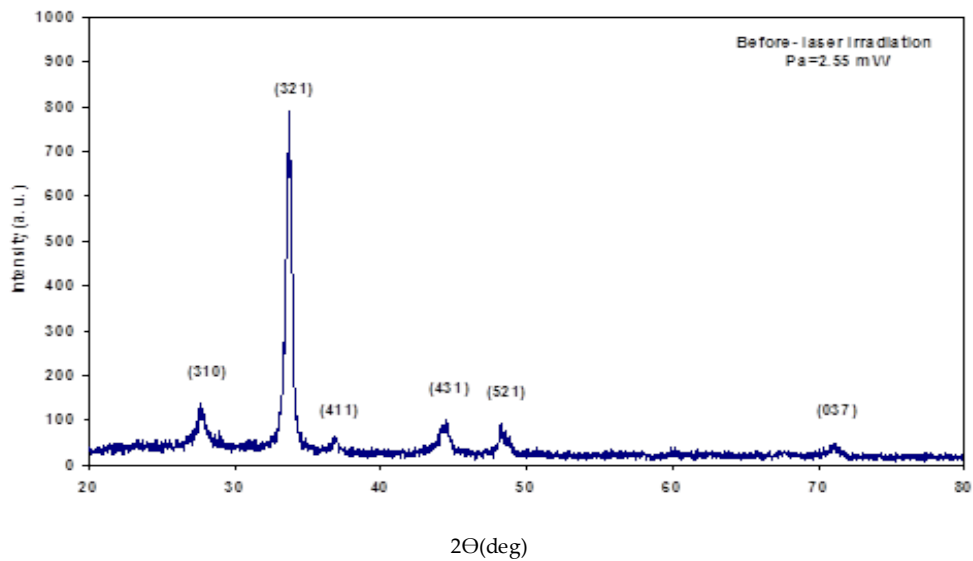
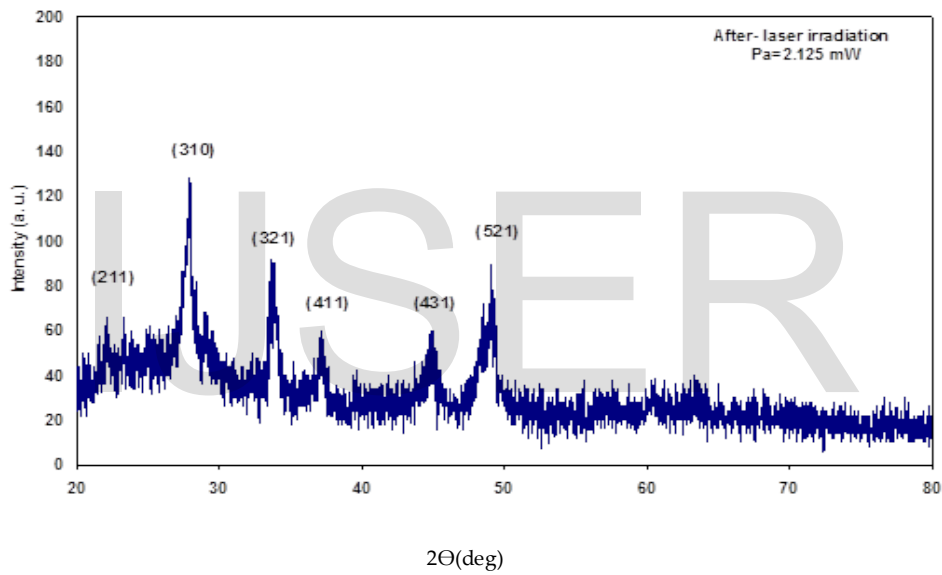
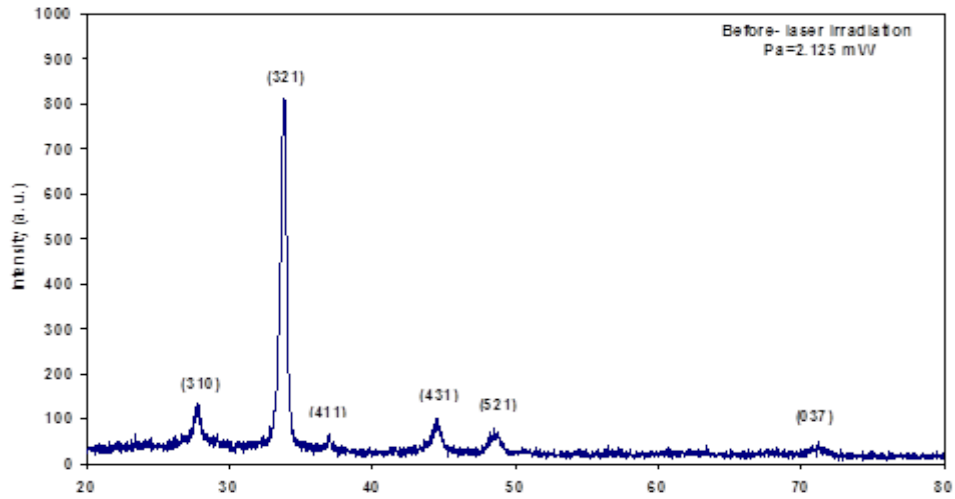
λ : is the X-ray wavelength (Å)

$\Delta_{(2\theta)}$: FWHM (degree)

θ : Bragg diffraction angle of the XRD peak (degree)

The calculated values are given in table (1).





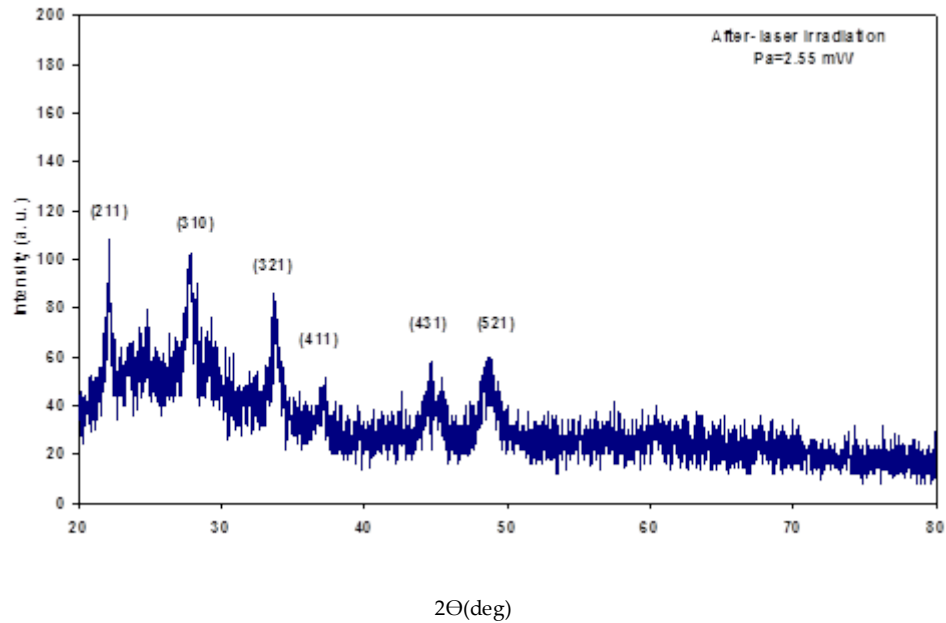


Figure (1) XRD before and after laser shot with different power average.

Grain Size (D)

The crystallite size of In_2O_3 films prepared at different power average. The films prepared before of laser irradiation showed the highest crystallite size and its value decreases after of laser irradiation as shown in table (1). The decrease in grain size indicates reduce the disorder, which may be due to residual compression stresses in the film or substitution of elements of small size for elements of large size. The XRD peaks can be widened (FWHM increase) by internal stress and defect when increasing after irradiation in the films, so the grain size decreases with increasing of power average [15]. On the other hand we can observe that the intensity of (321) peaks becomes weaker whereas peaks also become less intense at the laser power average increases. This indicates that the degree of crystallinity decreases with increasing power average in the film. The main calculations of the structural properties have been listed in the following:

Table (1) The obtained result of the structural parameters from XRD for Nanocrystalline In_2O_3 Films with different power average.

state	2 θ (Deg.)	FWHM (Deg.)	G.S (nm)	d_{hkl} Exp.(\AA)	d_{hkl} Std. (\AA)	hkl	phase	card No.
Before Pa=0.85 mW -glass	33.78	0.5	17.5	2.65	2.7	(321)	Cub. In_2O_3	44-1087
After Pa=0.85 mW -glass	33.77	0.58	15.0	2.65	2.7	(321)	Cub. In_2O_3	44-1087
Before Pa=1.70 mW -glass	33.82	0.54	16.17	2.65	2.7	(321)	Cub. In_2O_3	44-1087
After Pa=1.70 mW -glass	33.8	0.64	9.04	2.66	2.7	(321)	Cub. In_2O_3	44-1087
Before Pa=2.125 mW -glass	33.84	0.62	14.04	2.64	2.7	(321)	Cub. In_2O_3	44-1087
After Pa=2.125 mW -glass	33.66	1.02	8.93	2.7	2.7	(321)	Cub. In_2O_3	44-1087
Before Pa=2.55 mW -glass	33.72	0.6	14.61	2.65	2.7	(321)	Cub. In_2O_3	44-1087
After Pa=2.55 mW -glass	33.69	1.04	8.04	2.7	2.7	(321)	Cub. In_2O_3	44-1087

The (d) value, that is the interplanar spacing of (321) plane of the film was evaluated from the position of (321) peak from the XRD table (1). The observed (d) value is (2.64-2.7 \AA) which is in excellent agreement with the standard (d) value 2.7 \AA taken from the (JCPDS/44-1087) and the position of (321) peak taken from the XRD pattern is 33.66-33.84 $^\circ$ which is in agreement with the standard value 33.10 $^\circ$ taken from (JCPDS).

Lattice Constant (a)

The lattice constant (a) belong to the (321) plane as a preferred orientation for the In₂O₃ thin film for different power average with the agreement with the standard (JCPDS) values have been listed in table (2). The a-axis lengths increase when increasing power average of irradiation after from 0.85 to 2.55 mW, as in table (2).

Table (4.2): The values of lattice constant (a) of In₂O₃ films with different power average

State-glass	Pa=0.85 mW	Pa=1.70 mW	Pa=2.125 mW	Pa=2.55 mW
a (Å)-Before	9.91	9.91	9.90	9.91
a (Å)-After	9.91	9.93	10.1	10.1

Texture coefficient (T_c)

The value of texture coefficient of nanocrystalline In₂O₃ films are listed in table (3) .the texture coefficient is calculated using the relation: [15]

$$T_c(hkl) = \frac{I(hkl)/I_0(hkl)}{N_r^{-1} \sum I(hkl)/I_0(hkl)} \dots (3)$$

Where (I) is the measured intensity, (I₀) is the JCPDS standard intensity, (N_r) is the reflection number and (hkl) is Miller indices.

For crystal planes for all films, the value of texture coefficient decreased with increasing power average. The value of the texture coefficient indicates the maximum preferred orientation of the films along the diffraction plane, meaning that the decrease in preferred orientation is associated with decrease in the number of grains along that plane.

Number of layers (N_l)

The number of layers evaluated from different power average is listed in table (3). The number of layers is calculated using the relation: [15]

$$t = g.s \times N_l \dots \dots \dots (4)$$

Where (D) is a mean crystallite size or average grain size. The value of the number of layers increases with increase power average.

The Number of Crystallites Per Unit Area (N_o)

By using the nanocrystalline In_2O_3 films and grain size of the films prepared on glass substrate by spray pyrolysis technique at the substrate temperature (300°C) the number of crystallites per unit area was calculated and listed in table (3), and as in equation:

$$N_o = t / g \cdot s^3 \quad \text{cry}/(\text{m})^2 \quad \dots\dots\dots(5)$$

The values of the number of crystallites per unit area increases with increase power average.

Dislocation Density (δ)

The dislocation density is the measure of amount of defects in a crystal calculated using the equation:

$$\delta = \frac{1}{g \cdot s^2} \quad (\text{lines}/\text{cm}^2) \quad \dots\dots\dots(6)$$

Its obtained in the present work confirmed good crystallinity of the nanocrystalline In_2O_3 films fabricated by employing spray pyrolysis technique as shown in table (3). The values of dislocation density increases with increase power average.

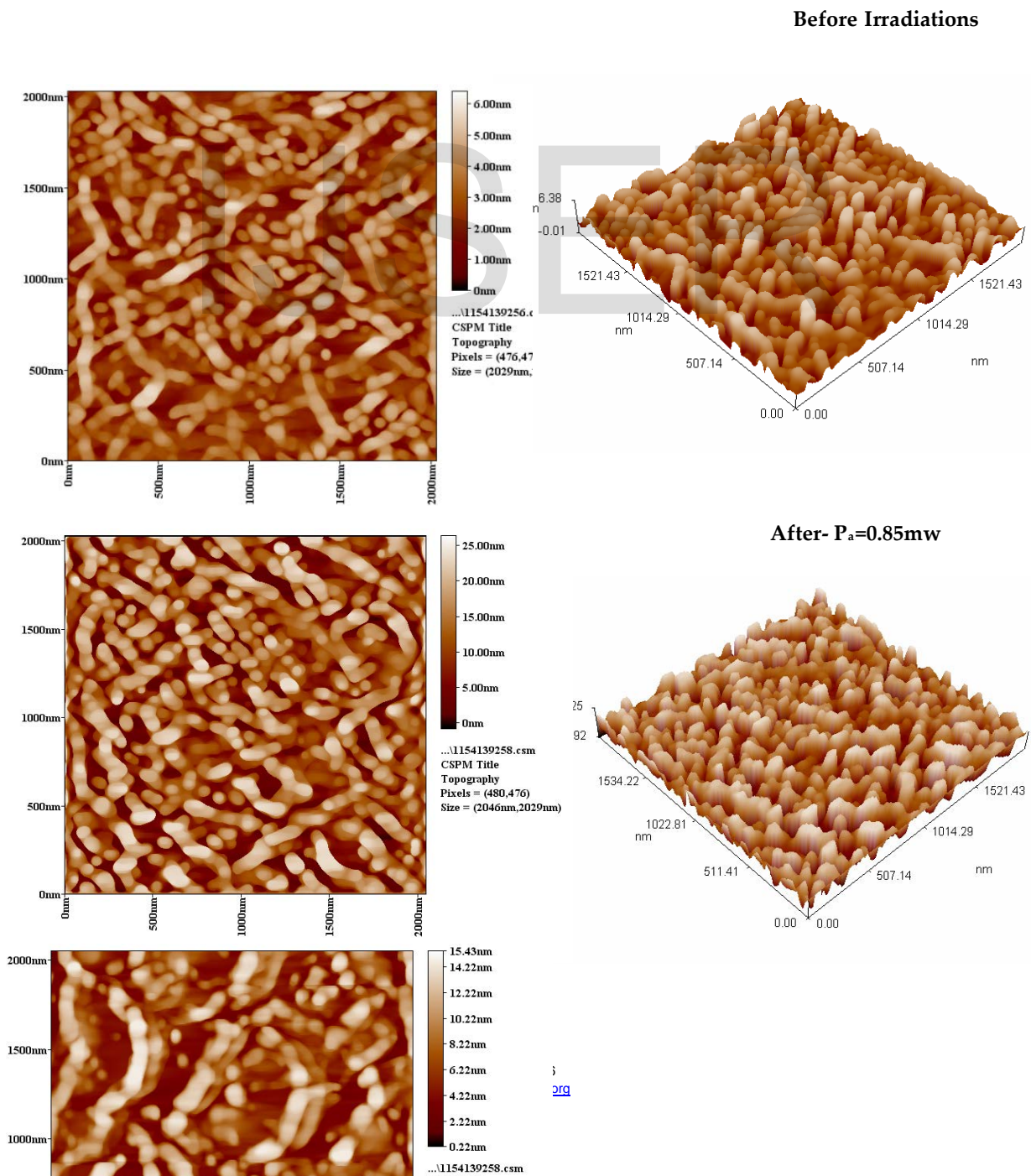
Table(3) some parameters that have been obtained from XRD diffraction with power average.

state	$N_i \times 10^{18}m^2$	$\delta \times 10^{14}m^2$	$N_o \times 10^{18}m^2$	Tc	hkl
Before 0.85mw- glass	11.42	3.2	0.037	2.80	(321)
After 0.85mw - glass	13.33	4.4	0.059	2.38	(321)
Before 1.70 mw-glass	12.36	3.8	0.047	3.23	(321)
After 1.70 mw-glass	22.12	12.2	0.27	2.98	(321)
Before 2.125 mw- glass	14.24	5.07	0.072	2.35	(321)
After 2.125 mw-glass	22.39	12.5	0.28	2.69	(321)
Before 2.55mw - glass	13.68	4.6	0.06	2.28	(321)
After 2.55 mw-glass	24.87	15.4	0.38	1.34	(321)

2. Atomic Force Microscopy (AFM)

The surface topography of the pristine and irradiated nanocrystalline In_2O_3 films were studied using Atomic Force Microscopy (AFM) Figure (2) shows the two and three dimensional micrograph in $(2 \times 2 \mu m^2)$ of In_2O_3 films with different power average (0.85, 1.70, 2.125, 2.55mw). The average grain size, root mean square roughness (RMS) and surface roughness of these films are shown in table (4). The AFM images of all samples displayed are granular structure. The average grain size decreasing from 49.0nm to 38.8nm after increasing the of power average of 0 to 2.55mW (after irradiation), these small grain sizes are uniformly distributed of shape and size

along the film surface, with tight packed grains is observed. the increasing power average lead to increased thermal energy, which enhances the mobility of the atoms on the surface further to form even larger grains, as they form smaller grains, the root mean square roughness and surface roughness also decreases due to the formation of deeper edges, or the surface roughness was decreasing as the power average increase. The roughness of the coated surface is an important parameter, where the surface roughness not only describes the light scattering but also gives an idea about the quality of the surface under investigation, in addition to providing some insight on the growth morphology. All the images appeared in figure (2) show homogeneous cluster distribution with nanocrystalline, also the energetic heavy ions provide sufficient energy for promoting the sputtering from the surface of the grains that leads to reduction in the grain size of nanocrystalline In_2O_3 Films [16].



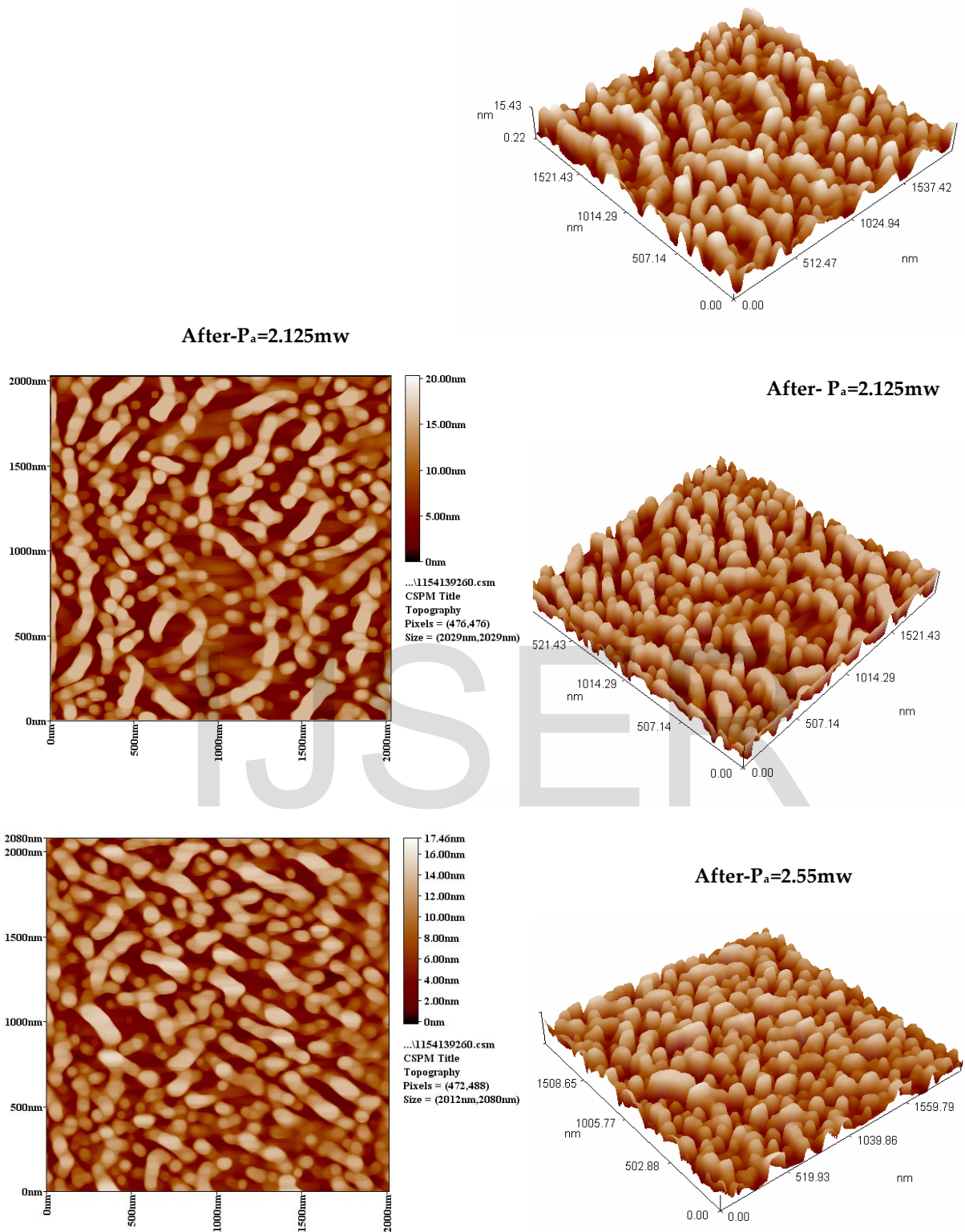


Figure (2) 2D and 3D AFM images of In_2O_3 films deposited at $300\text{ }^\circ\text{C}$ temperature with different power average.

Table (4) The values of AFM (before and after laser irradiated with different power average of In₂O₃ films).

Samples	Root Mean Square (nm)	Surface Roughness (nm)	Maximum height (nm)	Grain Size (nm)
P_a=0.0 Before irradiation	6.23	5.26	26.1	49.0
P_a=0.85mwAfter irradiation	4.65	4.12	16.0	45.26
P_a=1.70mwAfter irradiation	3.76	3.24	15.1	42.51
P_a=2.125mwAfter irradiation	3.18	2.74	12.9	40.09
P_a=2.55mwAfter irradiation	1.09	0.93	5.06	38.8

B. Sensing characteristics of the nanocrystalline In₂O₃ films sensors

The sensing for NO₂ gas properties of nanocrystalline In₂O₃ with investigated as a function of the operation temperature and also response and recovery time. In order to understand the temperature dependence on sensitivity to different power average of In₂O₃ thin films specimens for chemical sensing NO₂ gas with concentrations of about 6ppm. The sensing test was done using 3% NO₂ and 97 % air mixed ratio.

1. Effect of operating temperature

In general, the sensitivity of the sensor is affected by the operating temperature. The higher temperature enhances surface reaction of the thin films and gives higher sensitivity in a temperature range.

Figure (3) shows the sensitivity as functions of operation temperature from 150 to 350°C for the various power averages (0.85, 1.70, 2.125 and 2.55mW) of deposited In₂O₃ films under 6ppm NO₂ concentration. A rapid increase in sensitivity was observed as the operation temperature was increased to 300°C and reached a maximum for the P_a=1.70mw films and decreased thereafter with further increase in operation temperature. The variation of the temperature reveals resistance of

the film decreases as the temperature increases from room temperature to 150°C showing a typical negative temperature coefficient of resistance, due to thermal excitation of the charge carriers in semiconductor [17]. Above 150°C for different power average, sensor film displays positive temperature coefficient of film resistance as temperature increases further, which may be due to the saturation of the conduction band with electrons elevate from shallow donor levels caused by oxygen vacancies. At this point an increase in temperature leads to a decrease in electron mobility and a subsequent increase in films resistance. Similar observations are made by other research groups [18, 19]. At temperature higher than 150°C up to 300°C, the film resistance is greatly affected by the temperature variation because of the increase Sensitivity, probably due to the equilibrium obtained between the two competing processes: Thermal excitation because of irradiation of electrons and the oxygen adsorption. Finally, at temperature higher than 300°C the resistance decreases again, probably because of the dominant excitation of electrons and desorption of electron species [20]. So we believe that, the temperature range 150-300°C is suitable for sensor operation due to the small temperature dependence of the sensor. The sensitivity factor (S%) at various temperatures is calculated by equation:

$$S = \left| \frac{(R_g - R_a)}{NR_a} \right| \times 100\% \dots\dots\dots(7)$$

The relationship between power average, surface roughness and sensitivity's shown in table (5). The maximum sensitivity of the In₂O₃ film to NO₂ gas is found to be 64.12% at 300°C for power average 1.70mw. In₂O₃ thin films have no sensitivity for NO₂ Air mixed ratio for temperature less than 150°C. The sensitivity of the metal oxide semiconductor sensor is mainly determined by the interaction between the target gas and the surface of the sensor, the greater the surface area of the materials, the stronger the interaction between the adsorbed gases and the sensor surface, i.e. the higher the gas sensing sensitivity. It can be observed from AFM morphologies as shown in Table (5) that the surface roughness is small in the Pa=2.55mw film is lower Sense, While sensitivity increased with increasing surface roughness.

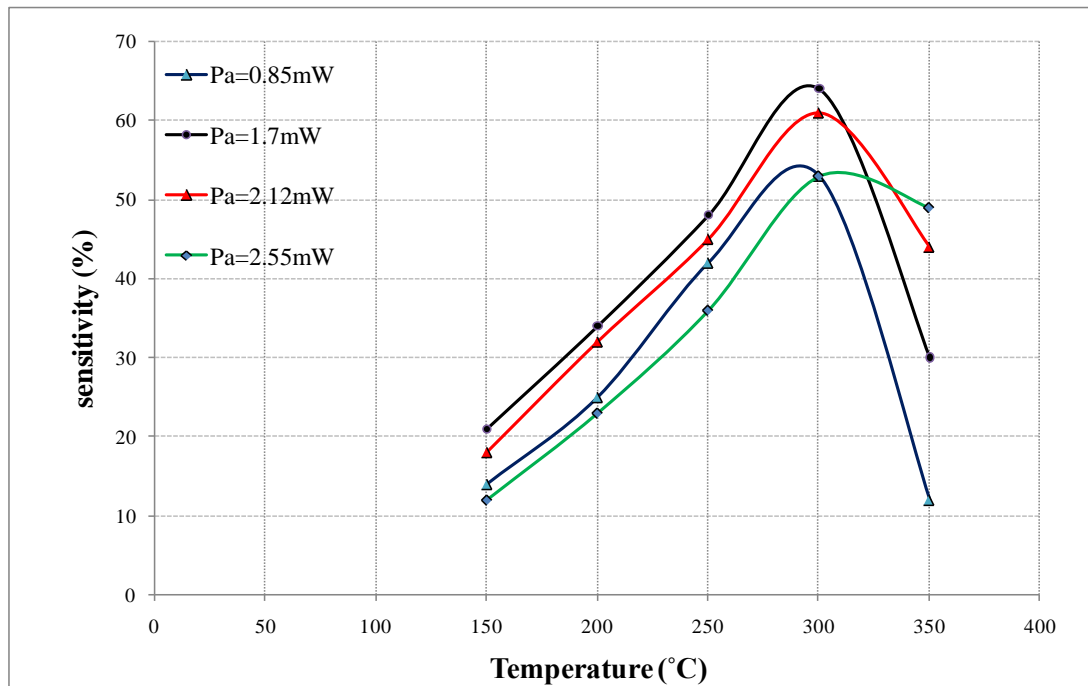


Figure (3) The variation of sensitivity with the operating temperature for different power average of the prepared In_2O_3 gas sensor .

Table (5) the values of sensitivity and surface roughness for In_2O_3 thin film with different power average.

averagepower (mW)	Sensitivity % at 300°C	Surface roughness (nm)
$P_a=0.85$	54.04	4.12
$P_a=1.70$	64.12	3.24
$P_a=2.125$	60.22	2.74
$P_a=2.55$	53.97	0.93

2. Response Time and Recovery Time

The response time and recovery time of thenanocrystalline In_2O_3 films towards 3% NO_2 : Air. The results are shown in figures (4) and (5), the relation between the response and recovery time with different power average of optimum operating temperature (150-300°C) of test gas. The response and recovery time ranging between increase and decrease with increasing power

average of films. The largest response and recovery time at this point were coming from power average (2.125mw) with grain size (40.09) nm at time (11.7sec) for response time and (23.4sec) for recovery time comparing to other samples. Both response and recovery time of the sensor have the same behavior as the NO₂ target gas. Both of them were increased and decreased with increasing power average which the lowest response and recovery times of (5.85s) and (9.0s)at power average (0.85mw)respectively are observed.All samples were tested at different power average and bias voltage (6 volt). The table (6) shown that response and recovery time with different power average.

Table (6) The values of response and recovery time with different power average.

Temperature (°C)	Power average (mw)	response time (sec)	recovery time (sec)
150	0.85	5.85	9
200	1.70	8.1	9.9
250	2.12	11.7	23.4
300	2.55	8.55	18.9

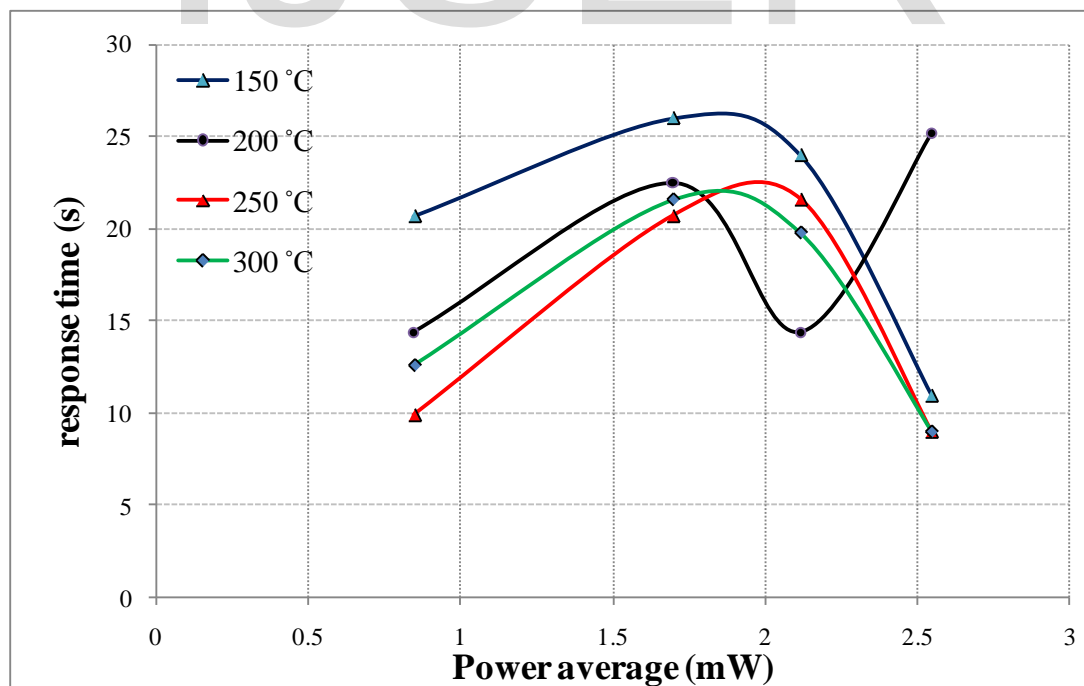


Figure (4) The variation of response time as function with different power average of the In₂O₃ gas sensor.

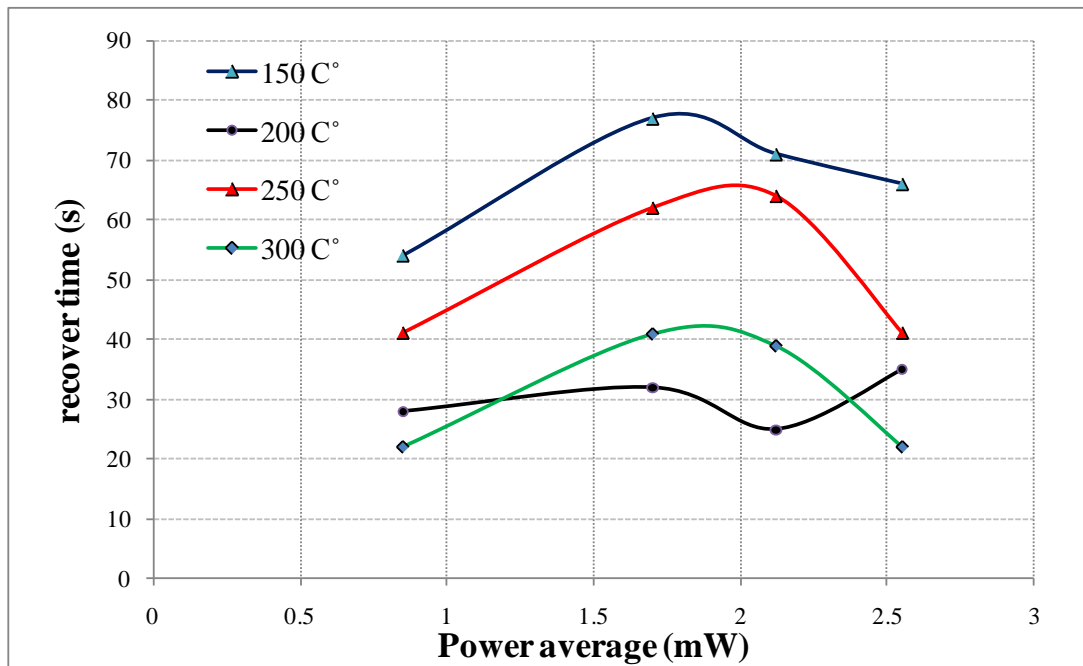


Figure (5) The variation of recovery time as function with different power average of the In_2O_3 gas sensor.

4. Conclusions

In_2O_3 Films Prepared by Chemical Spray Pyrolysis technique are irradiated with N_2 laser at 337 nm at substrate temperature of (300 °C) on glass substrate and different power average (0.85, 1.70, 2.125 and 2.55mW).

The XRD results showed that all films are polycrystalline in nature with a cubic structure and the preferred orientation was along the (321) plane for all films. The XRD peaks can be widened (FWHM increase) by internal stress and defect when increasing after irradiation in the films, so the grain size decreases with increasing of power average. The average grain size for In_2O_3 , estimated from XRD analysis. The power average (0.85mW) has highest grain size of about 17.5nm, and the power average (2.55mW) has minimum grain size of about 8.04nm, and was shown and have well identical with standard card (JCPDS) for cubic In_2O_3 crystal. Surface morphology by laser irradiation of nanocrystalline In_2O_3 films is change after irradiation.

The average of surface roughness (RS) and root mean square (RMS) was decreased after irradiation and grain size of In_2O_3 Film is decreased from 49 to 38.8 nm after irradiation with different power average.

Nanocrystalline In_2O_3 films sensors demonstrated high sensitivity and relatively fast to NO_2 gas. Thus, they exhibit showing excellent sensitivity for the maximum sensitivity is (64.12%) at at

300 °C for power average 1.70mw with grain size 42 nm. The largest response and recovery time at this point were coming from power average (2.125mw) at time 11.7sec for response time and 23.4 sec for recovery time, while fast response time (5.85s) and recovery time of (9.0s) at power average (0.85mw) comparing to other samples. The sensitivity of the In₂O₃ films the increase in the power average led to increasing in the sensitivity.

References

1. Granqvist, C.; Hultåker, A. Transparent and conducting ITO films: New developments and applications. *Thin Solid Films* 2002, 411, 1–5.
2. Park, S.K.; Han, J.I.; Kim, W.K.; Kwak, M.G. Deposition of indium-tin-oxide films on polymer substrates for application in plastic-based flat panel displays. *Thin Solid Films* 2001, 397, 49–55.
3. Geffroy, B.; le Roy, P.; Prat, C. Organic light-emitting diode (OLED) technology: Materials, devices and display technologies. *Polym. Int.* 2006, 55, 572–582.
4. Ginley, D.S.; Hosono, H.; Paine, D.C. *Handbook of Transparent Conductors*; Springer: New York, NY, USA 2010.
5. Klein, A.; Körber, C.; Wachau, A.; Säuberlich, F.; Gassenbauer, Y.; Harvey, S.P.; Proffit, D.E.; Mason, T.O. Transparent conducting oxides for photovoltaics: Manipulation of fermi level, work function and energy band alignment. *Materials* 2010, 3, 4892–4914.
6. Hans F. Wardenga, Mareike V. Frischbier, Monica Morales-Masis and Andreas Klein, In Situ Hall Effect Monitoring of Vacuum Annealing of In₂O₃:H Thin Films, *Materials* 2015, 8, 561-574.
7. Leonid I. Trakhtenberg, Seyed M. Navid Khatami, Genrikh N. Gerasimov, Olusegun J. Ilegbusi, Effect of Composition and Morphology on Sensor Properties of Aerosol Deposited Nanostructured ZnO+In₂O₃ Films, *Materials Sciences and Applications*, 2015, 6, 220-227.
8. Perednis, D. and Gauckler, L.J. (2005) Thin Film Deposition Using Spray Pyrolysis. *Journal of Electroceramics*, 14, 103-111.
9. Perednis, D. (2003) Thin Film Deposition by Spray Pyrolysis and the Application in Solid Oxide Fuel Cells. Ph.D. Thesis, Swiss Federal Institute of Technology, Zurich.
10. Trakhtenberg, L.I., Gerasimov, G.N., Gromov, V.F., Belysheva, T.V. and Ilegbusi, O.J. (2012) Effect of Composition on Sensing Properties of SnO₂ + In₂O₃ Mixed Nanostructured Films. *Sensors and Actuators B*, 169, 32-38.
11. Trakhtenberg, L.I., Gerasimov, G.N., Gromov, V.F., Belysheva, T.V. and Ilegbusi, O.J. (2013) Conductivity and Sensing Properties of In₂O₃ + ZnO Mixed Nanostructured Films: Effect of Composition and Temperature. *Sensors and Actuators B*, 187, 514-521.

12. Neri, G., Bonavita, A., Micali, G., Rizzo, G., Pinna, N., Niederberger, M. and Ba, J. (2008) Effect of the Chemical Composition on the Sensing Properties of $\text{In}_2\text{O}_3\text{-SnO}_2$ Nanoparticles Synthesized by a Non-Aqueous Method. *Sensors and Actuators B*, 130, 222-230.
13. A. Walsh, R. Catlow, "Structure, stability and work function of the low index surfaces of pure indium oxide and Sn-doped indium oxide (ITO) from density functional theory", *J. Mater. Chem.* 20 (2010), pp. 10438–10444.
14. Jing-Liang Li and Min Gu, "Gold-Nanoparticle-Enhanced Cancer Photothermal Therapy", *IEEE Journal of selected topics in quantum electronics*, 16(4),2010, pp.989 – 996.
15. Ali A. Yousif, "Preparation and Construction of Efficient Nanostructures Dopant ZnO Thin Films Prepared by Pulsed Laser Deposition for Gas Sensor", Ph.D. Thesis, Dept. of phys., University of Al-Mustansiriyah, (2010).
16. R. Kumaravel, V. Gokulakrishnan, K. Ramamurthi, Indra Sulania, D. Kanjilal, K. Asokan, D.K. Avasthi, "Effect of swift heavy ion irradiation on structural, optical and electrical properties of Cd_2SnO_4 thin films", *Nuclear Instruments and Methods in Physics Research Section B:Vol. 268, Issue 15*, (2010), pp.2391-2394.
17. A.S.Hasan, N.B.Hasan, A.J.Hayder, "study the doping effect with Mn on the morphology and optical properties of ZnS thin films prepared with pulsed laser deposition", the first scientific conference for college of science, University of karbala, 2013, pp. 18-25 .
18. N. H. Al-Hardan, M. J. Abdullah, A. Abdul Aziz, "Sensing mechanism of hydrogen gas sensor based on RF – sputtered ZnO thin films", *International journal of hydrogen energy* ,Vol. 35, (2010),pp. 4428 – 4434.
19. N. Abhijith, "Semiconducting metal oxide gas sensors", development and related instrumentation, M. Sc. Thesis, Indian Institute of Science, Bangalore, India, (2006).
20. N. H. Al-Hardan, M. J. Abdullah, A. Abdul Aziz, H. Ahmad, L. Y. Low, "ZnO thin films for VOC sensing applications", *Vacuum* ,Vol. 85, , (2010) pp. 101 – 106.